Supporting Information

Zhu et al. 10.1073/pnas.1018582108

SI Experimental Procedures.

RNA Design and Purification. pUC19-based plasmids encoding domain 3 of the *Plautia stali* intestine virus (PSIV) and Cricket paralysis virus (CrPV) intergenic region (IGR) internal ribosome entry site (IRES) between two ribozymes (1) and under control of a T7 promoter were generated using standard PCR and cloning methods [the original template plasmid containing the full-length PSIV IGR IRES was the kind gift of N. Nakashima (National Institute of Agrobiological Sciences, Ohwashi, Tsukuba, Ibaraki, Japan) and that of the CrPV IRES was a kind gift of P. Sarnow (Stanford University, Stanford, CA)]. These DNA plasmids were used as the template for PCR reactions to generate DNA containing the T7 promoter, the upstream hammerhead ribozyme, the 46-nt IRES sequence of Fig. 1*C*, and the *glmS* ribozyme (2). The RNAs were designed with an AUG codon immediately downstream of pseudoknot I (PK I) (Fig. 1*C*). In vitro transcriptions were conducted essentially as described (2) to include addition of glucosamine-6-phosphate to induce cleavage of the downstream ribozyme. The RNA then was purified by denaturing gel electrophoresis, eluted from the gel, concentrated, and washed as described (3, 4). The purified RNA was stored at −20 °C until used in crystallization trials.

Preparation of 70S Ribosomes. Ribosomes were isolated and purified from *Thermus thermophilus* as previously reported (5) and dissociated into subunits by incubating at 37 °C for 5 min in dissociation buffer D [25 mM Tris-OAc, pH 7.0, 100 mM KOAc, 1 mM $Mg(OAc)_2$]. Endogenously bound mRNAs, tRNAs, and protein factors were released from the ribosome under these conditions and further removed by three rounds of buffer exchange using Amicon Ultra-4 100K (Millipore) ultrafiltration devices at room temperature. The concentrate was then reassociated into complete 70S ribosomes by increasing the magnesium concentration to 25 mM in the presence of 3 mM spermine. A heat-activation step was performed by heating the reassociated ribosome solution at 65 °C for 5 min followed by slowly cooling to room temperature over 20 min. The buffer was then exchanged further to buffer E [25 mM Tris-OAc, pH 7.0, 50 mM KOAc, 10 mM NH_4OAc, 10 mM $Mg(OAc)_2$] by three rounds of ultrafiltration using Amicon Ultra-4 100K filters. The ribosome concentration was then adjusted to 20 mg/mL (8 mM) and aliquots were flash-frozen in liquid nitrogen and stored at −80 °C until further use.

1. Ferré-D'Amaré AR, Doudna JA (1996) Use of cis- and trans-ribozymes to remove 5′ and 3′ heterogeneities from milligrams of in vitro transcribed RNA. *Nucleic Acids Res* 24:977–978.
2. Keel AY, Easton LE, Lukavsky PJ, Kieft JS (2010) Large-scale native preparation of in vitro transcribed RNA. *Methods Enzymol* 469:3–25.
3. Costantino DA, Pfingsten JS, Rambo RP, Kieft JS (2008) tRNA-mRNA mimicry drives translation initiation from a viral IRES. *Nat Struct Mol Biol* 15:57–64.
4. Costantino D, Kieft JS (2005) A preformed compact ribosome-binding domain in the cricket paralysis-like virus IRES RNAs. *RNA* 11:332–343.
5. Laurberg M, et al. (2008) Structural basis for translation termination on the 70S ribosome. *Nature* 454:852–857.

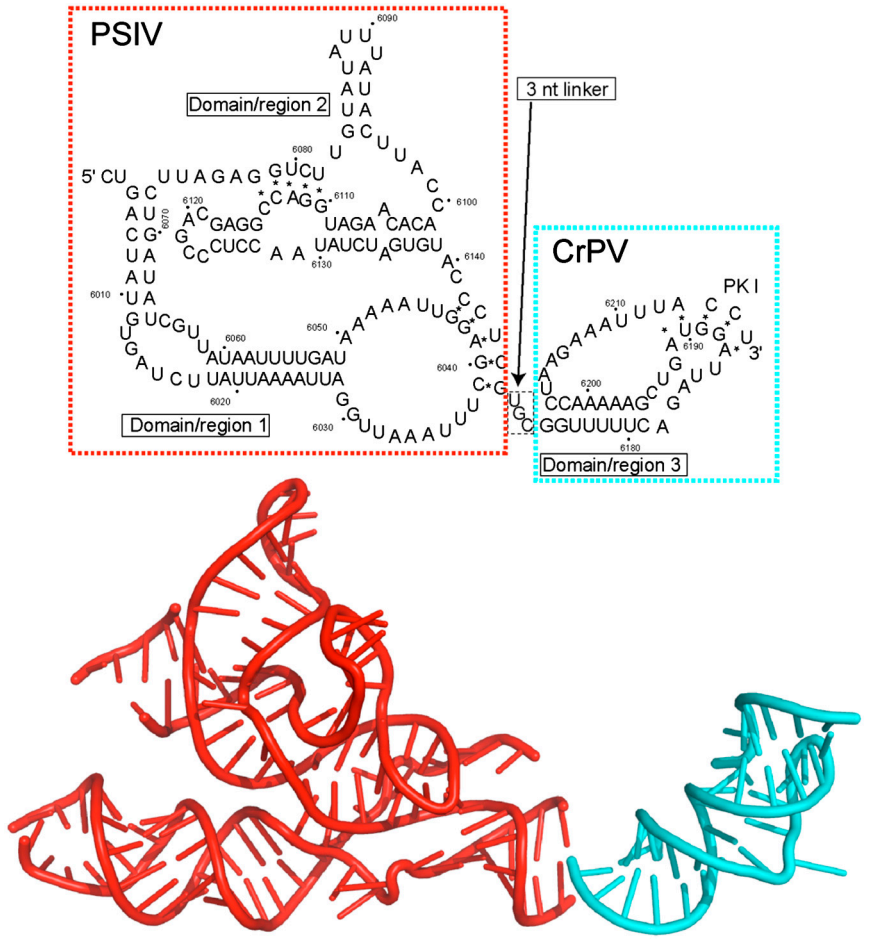

Fig. S1. Previously solved crystal structures of IGR IRES domains. The crystal structures of the unbound forms of domains 1 and 2 from the PSIV IGR IRES (1) and domain 3 from the CrPV IGR IRES (2) have been solved. (*Top*) Chimeric secondary structure showing these domains, with the PSIV domains 1 and 2 boxed in red and CrPV domain 3 boxed in cyan. Connecting these domains is a three-nucleotide linker that was not included in either crystal structure but that should span a distance of ~20 Å. (*Bottom*) Ribbon diagrams of the two structures are shown, with colors matching the boxes above. The structures are placed relative to one another in the approximate orientation in which they lie on the ribosome, based on cryo-EM structures (3, 4).

1. Pfingsten JS, Costantino DA, Kieft JS (2006) Structural basis for ribosome recruitment and manipulation by a viral IRES RNA. *Science* 314:1450–1454.
2. Costantino DA, Pfingsten JS, Rambo RP, Kieft JS (2008) tRNA-mRNA mimicry drives translation initiation from a viral IRES. *Nat Struct Mol Biol* 15:57–64.
3. Schuler M, et al. (2006) Structure of the ribosome-bound cricket paralysis virus IRES RNA. *Nat Struct Mol Biol* 13:1092–1096.
4. Kieft JS (2008) Viral IRES RNA structures and ribosome interactions. *Trends Biochem Sci* 33:274–283.

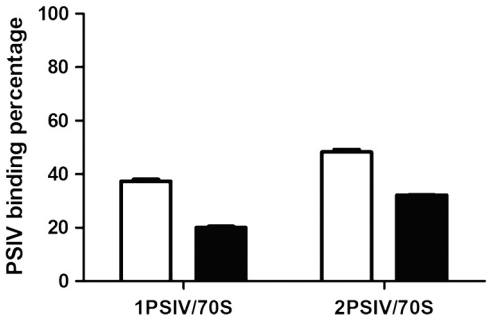

Fig. S2. Competition of tRNA for binding of PSIV IRES RNA to 70S ribosomes. A 1:1 (*Left*) or 2:1 (*Right*) molar ratio of [^{32}P]-labeled PSIV IRES RNA was bound to *T. thermophilus* 70S ribosomes in the absence (white bars) or presence (black bars) of a 1:1 molar ratio of deacylated elongator tRNA^{Met}. PSIV IRES binding was measured by filter binding, as described in *Experimental Procedures*.

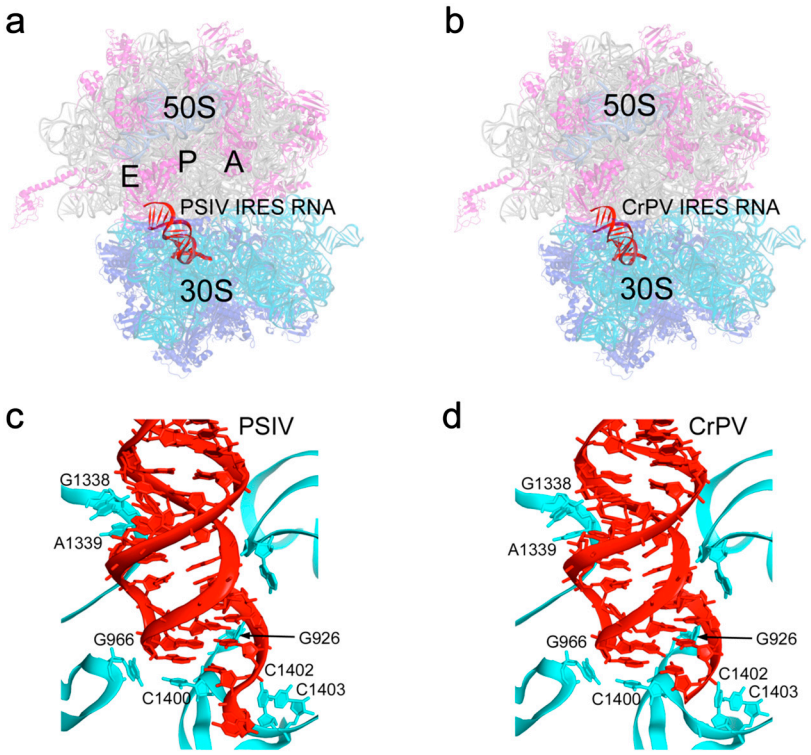

Fig. S3. (*A* and *B*) Positions of the PSIV and CrPV IRES domain 3 RNAs (red) in the P site of the *T. thermophilus* 70S ribosome. (*C* and *D*) Close-up views of the PSIV and CrPV domain 3 RNAs showing their contacts with the same features of 16S rRNA that interact with the P site tRNA anticodon stem-loop and P site codon (see Fig. 2*D*).

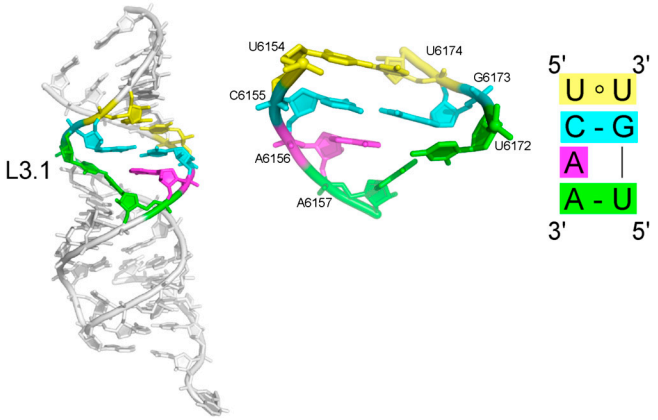

Fig. S4. Structure of L3.1 of the PSIV IGR IRES domain 3 when bound to a 70S ribosome. This loop lies between the coaxially stacked P3.1 and P3.2 helices (Fig. 1*C*). At left is the structure of the 70S ribosome-bound PSIV IGR IRES domain 3, with loop L3.1 indicated and nucleotides within that loop colored. At center is a close-up view of the structure of L3.1, with nucleotides colored to match the left panel and labeled. Within the loop, U6154 and U6174 form a U-U pair (yellow), C6155 and G6173 form a Watson–Crick C-G pair (cyan), A6157 and U6172 form a distorted Watson–Crick A-U pair, and A6156 stacks into the helix between the two Watson–Crick pairs. Note that in the structure of the unbound CrPV IGR IRES domain 3, the analogous nucleotide, A6182, was involved in crystal contacts and was extruded from the helix (Fig. 2*C*). At right is a diagram of the pairing and structure within L3.1. Although the loop contains a non-canonical base pair and an unpaired nucleotide, it results in only minor distortion from the geometry of an A-form RNA helix.

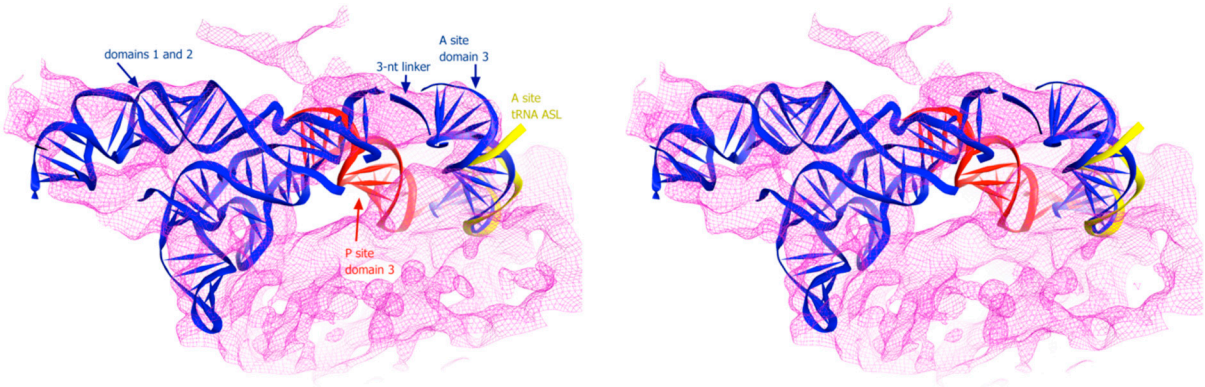

Fig. S5. Stereo view showing fitting of the three IGR IRES RNA domains to the 7.3-Å cryo-EM electron density map (1). Domain 3 makes a close fit to the density found in the small subunit A site. No density is observed in the small subunit P site, where the structure of domain 3 (red) is superimposed for comparison. The fit of domains 1 and 2 is essentially the same as originally described by Schuler et al. (1).

1. Schuler M, et al. (2006) Structure of the ribosome-bound cricket paralysis virus IRES RNA. *Nat Struct Mol Biol* 13:1092–1096.

Table S1. X-ray data collection and refinement statistics

Data collection	70S-PSIV	70S-CrPV
Space group	$P2_12_12_1$	$P2_12_12_1$
Cell dimensions		
a, *b*, *c* (Å)	211.9, 455.6, 618.0	210.7, 451.7, 614.3
α, β, γ (°)	90, 90, 90	90, 90, 90
Resolution (Å)	60.0–3.5 (3.6–3.5)*	70.0–3.4 (3.5–3.4)*
$R_{p.i.m.}(I)^{\dagger}$	0.1 (1.0)	0.1 (0.65)
$I/\sigma I$	8.8 (1.0)‡	11.4 (1.8)
Completeness (%)	100.0 (100.0)	97.5 (98.5)
Redundancy	23.6 (15.5)	6.7 (6.9)
Refinement		
Resolution (Å)	50.0–3.5	70.0–3.4
No. reflections	743,704	775,793
R_{work}/R_{free}	0.230/0.260	0.233/0.273
No. atoms	283,641	282,141
R.m.s deviations		
Bond lengths (Å)	0.005	0.009
Bond angles (°)	0.9	1.1

*Highest resolution shell is shown in parenthesis.
$^{\dagger}R_{p.i.m}(I)$ is a redundancy-independent merging *R*-factor (1).
$^{\ddagger}I/\sigma I = 2.0$ in the (3.7–3.8) resolution shell.

1. Weiss MS, Sicker T, Djinovic-Carugo K, Hilgenfeld R (2001) On the routine use of soft X-rays in macromolecular crystallography. *Acta Crystallogr D* 57:689–695.